

**Ground-state reference systems for expanding correlated fermions in one dimension**F. Heidrich-Meisner,<sup>1,2</sup> M. Rigol,<sup>3,4</sup> A. Muramatsu,<sup>5</sup> A. E. Feiguin,<sup>6</sup> and E. Dagotto<sup>2</sup><sup>1</sup>*Institut für Theoretische Physik C, RWTH Aachen University, 52056 Aachen, Germany*<sup>2</sup>*Materials Science and Technology Division, Oak Ridge National Laboratory, Oak Ridge, Tennessee 37831, USA**and Department of Physics and Astronomy, University of Tennessee, Knoxville, Tennessee 37996, USA*<sup>3</sup>*Department of Physics, University of California, Santa Cruz, California 95064, USA*<sup>4</sup>*Department of Physics, Georgetown University, Washington, D.C. 20057, USA*<sup>5</sup>*Institut für Theoretische Physik III, Universität Stuttgart, 70550 Stuttgart, Germany*<sup>6</sup>*Microsoft Project Q, University of California, Santa Barbara, California 93106, USA*

(Received 29 January 2008; revised manuscript received 28 April 2008; published 17 July 2008)

We study the sudden expansion of strongly correlated fermions in a one-dimensional lattice, utilizing the time-dependent density-matrix renormalization group method. Our focus is on the behavior of experimental observables such as the density, the momentum distribution function, and the density and spin structure factors. As our main result, we show that correlations in the transient regime can be accurately described by *equilibrium* reference systems. In addition, we find that the expansion from a Mott insulator produces distinctive peaks in the momentum distribution function at  $k \approx \pm \pi/2$ , accompanied by the onset of power-law correlations.

DOI: [10.1103/PhysRevA.78.013620](https://doi.org/10.1103/PhysRevA.78.013620)

PACS number(s): 03.75.Ss, 05.30.Fk, 05.70.Ln, 71.10.Pm

**I. INTRODUCTION**

The nonequilibrium properties of strongly correlated electron systems are a challenging subject in need of a better understanding. While experimental studies in this area face difficulties in the solid state context, ultracold quantum gases provide a controlled way to address this difficult issue. For this reason, recent experiments employing out-of-equilibrium cold atom gases in optical lattices, which allow the realization of model Hamiltonians for strongly correlated particles (for a review, see, e.g., Ref. [1]), have attracted considerable attention [2–4].

Among the fundamental questions recently addressed in these experiments is the issue of thermalization in isolated quantum systems [2,5–14]. In the transient regime, quantum quenches have been shown to induce a collapse and revival of coherence properties [3], and transport measurements in different lattice systems have unveiled the intriguing consequences of strong correlations [4]. The important effects of interactions have been observed in the expansion of bosons in one-dimensional (1D) lattices as well [15–19]. In the expansion from a Mott insulator (MI) state, quasicondensates at finite momenta emerge [15], while in the hard-core regime, the expansion from a superfluid state leads to the dynamical fermionization of the bosonic momentum distribution function (MDF) [16]. The latter is a generic feature of the expansion of harmonically trapped hard-core bosons in the absence of a lattice [20]. In addition, it has been shown in Ref. [21] that independently of the initial interaction strength, a freely expanding Lieb-Liniger gas always enters a strongly correlated (hard-core-like) regime. The expansion dynamics of strongly correlated fermions, which due to the spin degree of freedom is expected to be richer, has not yet been addressed, and it is the objective of this work.

Concretely, we study the expansion of two-component interacting fermions in a 1D lattice. The ground-state physics of these systems is characterized by a Tomonaga-Luttinger

(TL) state with power-law decaying correlations at any incommensurate filling. At half-filling, a charge gap opens and the system exhibits quasi-long-range antiferromagnetic correlations [22]. Here, we wish to elucidate how the initial state of the system, being either MI or TL, affects the expansion process. Identifying distinctive features for the MI is of much interest to experimentalists in the search for the fermionic MI state. However, our main objective is to shed light on the relation, if any, between these out-of-equilibrium systems and their equilibrium counterparts. As the main result of this work, we provide evidence that correlations measured in nonequilibrium are quantitatively described by appropriately chosen equilibrium reference systems.

The outline of the paper is the following. First, we describe the model and the numerical procedure in Sec. II. Section III contains our results on the time evolution of density profiles and the momentum distribution function for both TL and MI initial states. In Sec. IV, we investigate the possible relation to equilibrium systems, and we present a comparative analysis of spin and charge correlation functions. We also comment on the validity of our findings in other models, such as the Hubbard chain with a nearest-neighbor repulsion, which renders the model nonintegrable. We conclude with a summary of our results contained in Sec. V.

**II. MODEL AND NUMERICAL METHOD**

The nonequilibrium dynamics is analyzed using the adaptive time-dependent density-matrix renormalization group method (tDMRG) [23]. We consider the 1D Hubbard model with nearest-neighbor hopping  $t$  and an on-site Coulomb repulsion  $U$  as follows:

$$H_0 = -t \sum_{l=1}^{N-1} (c_{l+1,\sigma}^\dagger c_{l,\sigma} + \text{H.c.}) + U \sum_{l=1}^N n_{l,\uparrow} n_{l,\downarrow}. \quad (1)$$

$c_{l,\sigma}^\dagger (c_{l,\sigma})$  is a fermion creation (annihilation) operator acting on site  $l$ , with (pseudo)spin index  $\sigma = \uparrow, \downarrow$ ,  $n_{l,\sigma} = c_{l,\sigma}^\dagger c_{l,\sigma}$  is the

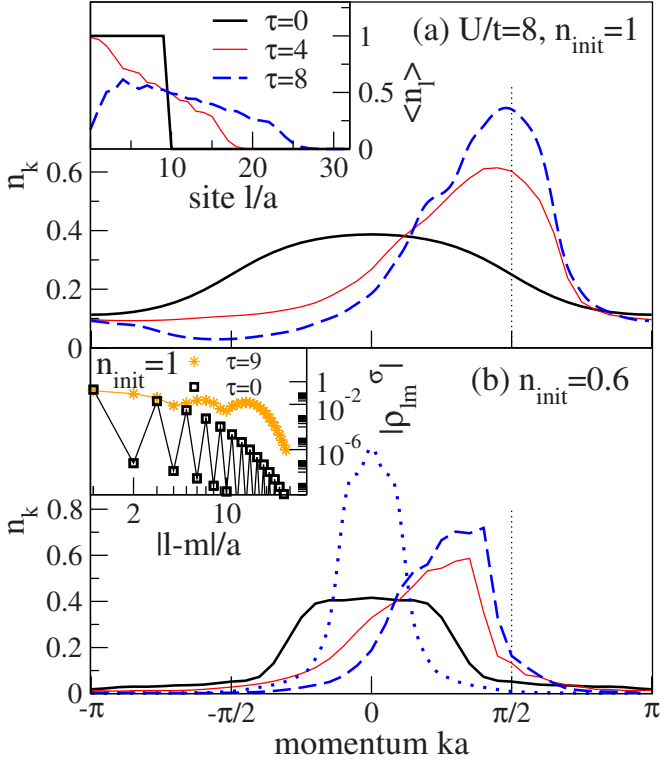


FIG. 1. (Color online) Expansion from a (a) MI ( $n_{\text{init}}=1$ ; main panel: MDF; inset: density); (b) TL ( $n_{\text{init}}=0.6$ ); both at  $U=8t$  and plotted at times  $\tau=0, 4, 8$ . Note that at  $\tau \geq 8$  and before the right boundary is reached, the MDF exhibits only small changes. Dotted line in (b): MDF of a reference system (see the text in Sec. IV A for details) with  $\langle n_i \rangle_{\text{ref}, \tau} = \langle n_i(\tau=8) \rangle$ . Inset in (b): Decay of one-particle correlations during the expansion of the MI. The  $\tau=0$  curve is for a  $N=50$  system at half-filling. The dotted vertical lines in (a) and (b) denote  $k=\pi/2$ .

corresponding density operator, and we define  $n_l = \sum_{\sigma} n_{l,\sigma}$ .  $N$  denotes the number of sites,  $a$  is the lattice constant, and open boundary conditions are imposed. We prepare an initial state with a filling  $n_{\text{init}}$  that is nonvanishing in only a portion of the system by applying a confining box potential  $H_{\text{conf}} = \sum_{l=1}^N \epsilon_l n_l$ . Hence, we have  $H = H_0 + H_{\text{conf}}$ , with  $\epsilon_l = 10^6 t$  for  $l \notin [l_0, l_1]$  and  $\epsilon_l = 0$  otherwise. At time  $\tau=0$ , we turn off  $H_{\text{conf}}$ .  $\tau$  is given in units of  $1/t$ ; we set  $\hbar$  to unity.

In our tDMRG runs we use a third-order Trotter-Suzuki time-evolution scheme with a time step of  $\Delta\tau=0.005$ . The discarded weight during the time evolution is kept below  $10^{-8}$ . To simulate the longest time scales possible on a given system size before the particles are reflected at the boundaries, we select an asymmetric setup and, hence, particles can only expand into one direction. We have checked that the same overall picture is observed in symmetric setups (see also Ref. [15]).

### III. MOMENTUM DISTRIBUTION FUNCTION

We first discuss the properties of the MDF  $n_k$ , computed from  $n_k = (1/N) \sum_{l,m,\sigma} \exp[-ik(l-m)] \rho_{lm}^{\sigma}$ , where  $\rho_{lm}^{\sigma} = \langle c_{l,\sigma}^{\dagger} c_{m,\sigma} \rangle$  is the one-particle density matrix. In Fig. 1(a), we

show the evolution of  $n_k$  (main panel) and the density  $\langle n_i \rangle$  (inset) for an initial MI state. The main panel reveals a peculiar behavior of  $n_k$ : as the Mott insulator melts, a peak develops at a finite momentum  $k_p$ . We further find that, for  $U$  larger than the bandwidth  $W=4t$ ,  $k_p$  closely approaches  $\pi/2$ . This behavior resembles that of hard- and soft-core bosons [15]. Qualitatively, we understand this in terms of an energy argument: in the MI state with  $U \gg W$ , the total kinetic energy is close to zero. Hence, particles emitted into an empty lattice have a small average kinetic energy corresponding to a momentum  $\pi/2$ . As the Fermi statistics prohibits quasicondensation into a single momentum state,  $n_k$  becomes a broad function around  $k_p \approx \pi/2$ .

While the initial MI state is characterized by an exponential decay of one-particle correlations, i.e.,  $|\rho_{lm}^{\sigma}| \sim \exp(-|l-m|/\xi)$ ,  $\xi = \text{const}$ , we find that during the expansion, the system develops power-law correlations. In the inset of Fig. 1(b), we compare the  $|\rho_{lm}^{\sigma}|$  of a MI in equilibrium with the correlations that emerge during its expansion, measured within the moving cloud. The inset reveals the weak decay of correlations during the expansion, consistent with a power law. One may associate the dynamical emergence of this power law with a *metallization* of the moving cloud, which, after the melting of the MI, starts behaving as an inhomogeneous metal. As of now, our numerical analysis is restricted to a small number of particles and time scales of  $\tau \sim 15$  only, which prevents us from extracting, e.g., exponents of the power laws. Note, though, that in the case of free fermions expanding from an insulating state with  $n_{\text{init}}=1$ , i.e., a state with no off-diagonal correlations, the emergence of power laws has been established for a large number of particles and hence over substantially larger distances than in the present work [24].

In the main panel of Fig. 1(b), we show the evolution of the MDF starting from a TL state with  $n_{\text{init}} < 1$ . In this case, the initial state has a well-defined Fermi momentum and a power-law decay of correlations [22]. Such decay is preserved during the expansion. Moreover,  $n_k$  also exhibits a peak, but at a momentum  $k_p < \pi/2$  ( $k_p$  increases as  $n_{\text{init}} \rightarrow 1$ ). Another property of this peak, distinguishing it from the peak formed after the melting of the MI, is that it exhibits a much sharper edge at the large momentum side, reminiscent of a Fermi edge.

From the previous analysis, we conclude that if  $n_k$  could be experimentally studied during the expansion in the strongly correlated regime, then the emergence of peaks at  $k = \pm \pi/2$  in the fermionic MDF would serve to identify the presence of a Mott insulator in the initial state. The experimental challenge is to independently control the trapping potential and the lattice [25–27]. This has been achieved in the experimental study of disordered ultracold Bose gases in both 1D optical lattices [26] and homogeneous 1D systems [27].

At this point we would like to emphasize that the physics of our expanding system is different from the one found in theoretical studies of strongly correlated systems in 1D lattices undergoing a relaxation following a quantum quench [5,9,10]. In the latter, correlations have been found to decay faster than with a power law (sometimes clearly exponentially) [5,7,9,10], while in our moving clouds we find power-

law decaying correlations [inset of Fig. 1(b)]. In addition, after the relaxation to a steady state, one can ask the question of what statistical ensemble may best describe physical observables, but here we are solely concerned with the transient regime, i.e., a regime in which statistical ensembles do not provide us with insights into the behavior of physical observables.

#### IV. GROUND-STATE REFERENCE SYSTEMS

##### A. Construction of reference systems

Our results thus far have singled out a noticeable property of these systems during their expansion: independently of the initial ground state, power laws are observed in the nonequilibrium dynamics. In 1D systems in equilibrium, power-law correlations are only seen in the ground state, as finite temperatures introduce a cutoff at large distances, followed by an exponential decay [22]. Hence, one may wonder whether a system out of equilibrium can in some way resemble the ground state of a system in equilibrium. A natural choice for such a reference state is the ground state of a system that has exactly the same density distribution as the time evolving state, i.e.,

$$\langle n_l \rangle_{\text{ref},\tau} = \langle n_l(\tau) \rangle, \quad (2)$$

for all sites  $l$ . Hence, a reference system has to be determined at each given time. We construct such reference states by self-consistently computing a set of on-site energies  $\epsilon_l$  in

$$H_{\text{ref}} = H_0 + \sum_{l=1}^N \epsilon_l n_l, \quad (3)$$

with  $H_0$  from Eq. (1) such that at a desired time, the density profile  $\langle n_l(\tau) \rangle$  is reproduced, while keeping  $t$  and  $U$  fixed. Once the density has converged within an error of

$$\delta n_\tau = \sum_l |\langle n_l(\tau) \rangle - \langle n_l \rangle_{\text{ref},\tau}| / \sum_l \langle n_l(\tau) \rangle < 10^{-3}, \quad (4)$$

we compare quantities of interest in both systems.

##### B. Spin and charge structure factor

We now turn to the comparative analysis of correlation functions. We compute the spin-spin ( $S_k$ ) and density-density ( $N_k$ ) structure factors, which are the Fourier transforms of the spin-spin ( $S_{lm} = \langle S_l^z S_m^z \rangle$ ) and density-density ( $N_{lm} = \langle n_l n_m \rangle - \langle n_l \rangle \langle n_m \rangle$ ) correlations, respectively. The spin operator is defined as  $S_l^z = (n_{l,\uparrow} - n_{l,\downarrow})/2$ . In equilibrium and for a homogeneous system,  $S_k$  peaks at  $2k_F$  while  $N_k$  exhibits a kink at  $4k_F$  [22], where  $k_F = \pi n/2$  is the Fermi momentum. Consistently, for the two cases  $n_{\text{init}}=1$  and  $n_{\text{init}}=0.6$  shown in Figs. 2(a) and 2(c), respectively,  $S_k(\tau=0)$  (dotted lines) peaks at  $k=\pi$  and  $k=\pi/6$ , while  $N_k$  in the case of  $n_{\text{init}}=0.6$  has a weak kink at  $k=2\pi/6$  [dotted line in Fig. 2(d)]. During the expansion, the peak in  $S_k$  shifts to smaller momenta and the maximum is less sharp, as shown in Figs. 2(a) and 2(c) (solid lines). Qualitatively, we understand this behavior in terms of the decrease of the average density during the expansion into the initially empty lattice, giving rise to a shift of the  $2k_F$

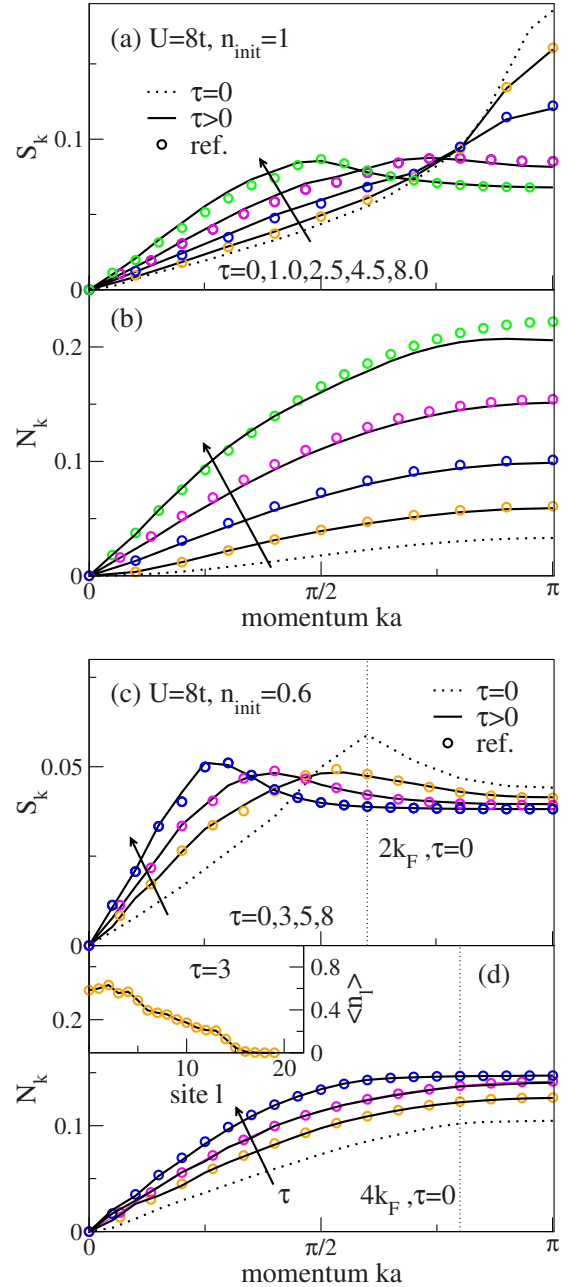


FIG. 2. (Color online) Time evolution (solid lines) of [(a),(c)]  $S_k$  and [(b),(d)]  $N_k$  for the expansion with [(a),(b)]  $n_{\text{init}}=1$  at times  $\tau=0, 1.0, 2.5, 4.5, 8.0$ ; and [(c),(d)]:  $n_{\text{init}}=0.6$  at times  $\tau=0, 3, 5, 8$  (all at  $U=8t$ ). Thick, dotted lines denote the  $\tau=0$  results and the arrows indicate increasing time. The vertical dotted lines in (c) and (d) are  $2k_F$  and  $4k_F$ , respectively. The same quantities,  $S_k$  and  $N_k$ , for reference systems (see the text for details) are included (circles). Inset in (d): density profile at time  $\tau=3$ .

peak in  $S_k$  and a broadening due to the inhomogeneity. Further, we propose an operational definition of a Fermi-momentum  $k_F^\tau$  in the expanding clouds by taking the position of the peak in  $S_k$ , yielding  $2k_F^\tau$ . This supports the use of the term “metallization” for the process that fermions escaping from a MI undergo.

The density correlation  $N_k$  does not show any particular features during the time evolution, as the kink is washed out

due to the inhomogeneity.  $N_k$  increases monotonously with time, reflecting an increase of the overall charge fluctuations, due to the closing of the charge gap as the MI melts.

Our most remarkable finding, and thus the key result of this work, is the excellent agreement seen in Fig. 2 for  $S_k$  and  $N_k$  between the expanding cloud—a genuine nonequilibrium situation—and the inhomogeneous reference systems, which are in their ground state (circles in Fig. 2). We are therefore led to conclude that, during the expansion, spin and charge correlations out of equilibrium are, to a very good approximation, the same functionals of the density as the ones in equilibrium systems in the ground state.

### C. Time evolution of kinetic and potential energy

Intuitively, we expect that our way of preparing the reference systems must yield properties similar to those of the moving clouds on short time scales. However, the agreement between the clouds and the equilibrium systems exists both at short and long times, and is thus preserved during the expansion into the empty lattice. A noticeable difference exists between  $n_k$  of the moving clouds and  $n_k$  of the corresponding reference systems. As discussed before,  $n_k$  of the expanding cloud has a finite-momentum maximum, which is also present in the symmetric expansion, while  $n_k$  of the reference system in its ground state is symmetric around  $k=0$  [see the dotted line in Fig. 1(b)]. Hence, observables related to  $n_k$  cannot be accounted for with this procedure.

Our previous findings on the spin and density structure factors may seem puzzling: at any given time, the sum of the kinetic energy  $T_{\text{kin}}$  and the interaction energy  $E_{\text{int}}$  of the time-evolving state is much higher than the energy of the reference system, which, having the same density profile, is in its ground state. This difference grows with time. In the case of  $n_{\text{init}}=0.6$  and  $U=8t$ , we have  $E_0=T_{\text{kin}}+E_{\text{int}}=-6.86t$ , which of course is a constant in time. At  $\tau=8$ , this splits into  $T_{\text{kin}}=-t\sum_{l,\sigma}\langle c_{l+1,\sigma}^\dagger c_{l,\sigma} + \text{H.c.} \rangle = -6.97t$  and  $E_{\text{int}}=U\sum_l \langle n_{l,\uparrow} n_{l,\downarrow} \rangle = 0.11t$ . In contrast, for the reference system, we find  $T_{\text{kin}}^{\text{ref}} = -10.93t$ , and  $E_{\text{int}}^{\text{ref}} = 0.18t$ , adding up to  $E_0^{\text{ref}} = -10.75t$ . Thus, the main difference is due to the kinetic energies.

We argue that both systems can be related by a Galilean transformation and, thus, understand why their structure factors are similar. This means that the difference between the kinetic energies  $T_{\text{kin}}$  and  $T_{\text{kin}}^{\text{ref}}$  is mainly due to the average momentum of the moving cloud [ $k_0 = \sum_k k n_k / \sum_k n_k$ ], i.e., that  $T_{\text{kin}}^{\text{ref}} \approx T_{\text{kin}}^{\text{Gal}}$ , the latter being the kinetic energy of the particles in a reference frame moving with the cloud. To prove this, we first notice that, using the MDF, the kinetic energy can be estimated as

$$T_{\text{kin}} = \sum_k n_k \epsilon_k^0, \quad (5)$$

where  $\epsilon_k^0 = -2t \cos k$  is the dispersion relation in the noninteracting case. This assumption leads to  $T_{\text{kin}} \approx -6.97t$  and  $T_{\text{kin}}^{\text{ref}} \approx -10.93t$ , as estimates for the kinetic energy of the expanding and reference systems at  $\tau=8$  ( $n_{\text{init}}=0.6$ ,  $U=8t$ ), respectively. Both values are very close to the exact results presented before. We then compute  $T_{\text{kin}}^{\text{Gal}} = \sum_k n_k \epsilon_{k-k_0}^0 = -10.15t \approx T_{\text{kin}}^{\text{ref}}$  at  $\tau=8$ , which corroborates our interpreta-

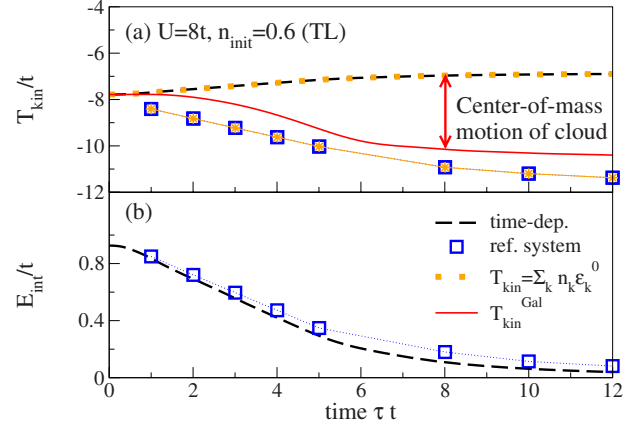


FIG. 3. (Color online) Time evolution of (a) the kinetic energy  $T_{\text{kin}}$  and (b) the potential energy  $E_{\text{int}}$  for the expansion from an initial TL state with  $U=8t$ ,  $n_{\text{init}}=0.6$  (dashed lines), and the corresponding reference systems (squares). Panel (a) further shows the kinetic energy of the cloud and of the reference systems as estimated from Eq. (5) (thick dotted line and stars, respectively) as well as our approximate results for the kinetic energy  $T_{\text{kin}}^{\text{Gal}}$  associated with the center-of-mass motion of the cloud [solid line in (a)]. See the text in Sec. IV C for definitions and details.

tion: the energy difference is mostly due to the finite momentum of the cloud, and not due to contributions of the internal kinetic or interaction energy. This picture is further supported by Fig. 3 that contains the time evolution for  $T_{\text{kin}}$ ,  $E_{\text{int}}$ ,  $T_{\text{kin}}^{\text{ref}}$ , and  $T_{\text{kin}}^{\text{Gal}}$  for the parameters discussed in this section.

### D. Breakdown of the ground-state reference-system description

It is next important to identify conditions for a breakdown of the reference-system description. To this end, we study the relative difference between the time-dependent and the reference systems' density structure factors,

$$\delta N_{k,\tau} = \frac{\sum_k |N_k(\tau) - N_k^{\text{ref}}|}{\sum_k N_k(\tau)}. \quad (6)$$

The corresponding errors in  $S_k$  are smaller than those in  $N_k$ , and we thus concentrate on the latter. Let us start with the initial TL. We consider two cases: first,  $n_{\text{init}} < 1$  in a box trap [see Fig. 2(d)]. Second, as such a setup is more realistic to account for experiments, we follow the evolution of fermions escaping from a harmonic trap  $V_{\text{trap}} \sum_l (l)^2 n_l$ . From the results displayed in Fig. 4(a), our key observation is that  $\delta N_{k,\tau} \lesssim 0.02$  remains very small in both cases. Hence, for an initial TL state and for both  $N_k$  and  $S_k$ , the description given by the equilibrium systems is very good up to the largest times simulated.

We next turn to the case of an initial MI region, and present results in Fig. 4(b) for  $U=8t, 20t, \infty$ . The  $U=\infty$  case is treated with exact diagonalization, after mapping the charge sector of our two-component fermion system to spinless fermions [22]. A behavior similar to the TL case is found at times  $\tau \lesssim 5$ , with  $\delta N_{k,\tau} \lesssim 0.04$ . However, for times after the melting of the MI region [ $\tau \gtrsim 5$ , see the inset in Fig. 4(b)], a substantial increase of  $\delta N_{k,\tau}$  becomes evident, as shown in



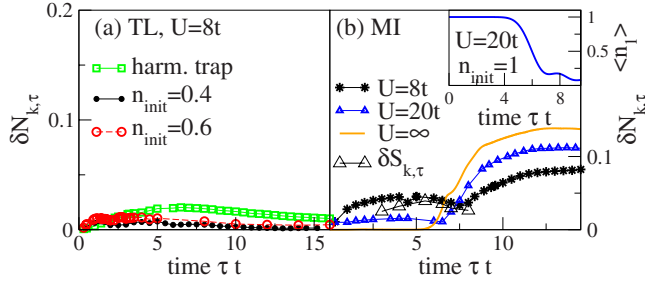


FIG. 4. (Color online) Relative deviation of the density structure factor vs time [see Eq. (6)], for (a)  $n_{\text{init}}=0.4, 0.6$  and a harmonic trap (8 fermions,  $V_{\text{trap}}=0.02t$ ,  $U=8t$ ) and (b)  $n_{\text{init}}=1$  ( $U/t=8, 20, \infty$ ). We estimate our calculation of  $\delta N_{k,\tau}$  to have an accuracy of  $\pm 0.01$  in the worst case. Inset in (b): density in the leftmost site vs time for  $U=20t$ .

Fig. 4(b). Thus, for the MI expansion, reference systems work well only up to the point at which the Mott insulator totally melts.

This deviation of the time-dependent data from the reference systems is associated to the appearance of particular coherence properties in the portion left behind by the moving cloud after the melting of the MI, a feature that is not captured by the reference systems. To substantiate this interpretation, we present results for the decay of  $N_{ij}$  in the  $U=\infty$  limit in Fig. 5. In that limit, we are able to exactly treat arbitrary time scales for both a large number of particles and a large system size. The data displayed in Fig. 5 are for 500

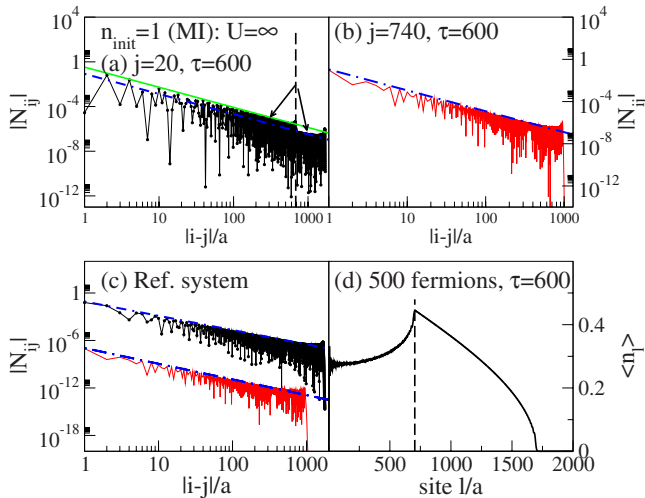


FIG. 5. (Color online)  $U=\infty$ , 500 particles,  $n_{\text{init}}=1$ . (a) Decay of  $|N_{ij}|$  at time  $\tau=600$  for  $j=20$  (solid line with squares). The dashed lines are fits to the envelope of  $|N_{ij}|$  using  $f(|i-j|)=\alpha|i-j|^{-\beta}$ . Note that two regions appear that are described by the same exponent  $\beta$ , but a different prefactor  $\alpha$ . (b) The same as in (a), but for  $j=740$  (solid line). Note that we plot correlations for  $i>j$  only. (c) Density-density correlations measured in the reference system for  $\tau=600$ , with  $j=20$  (solid line with squares) and  $j=740$  (solid lines). The latter curve has been offset for clarity. The dashed-dotted lines are the fits from panels (a) and (b). (d) Density profile at time  $\tau=600$ . Vertical, dashed lines in (a) and (d) mark  $i=705$ , separating the regions with different prefactors in the power-law decay of  $|N_{ij}|$  at the time  $\tau=600$  considered in this plot.

spinless fermions expanding from a MI region into a lattice of 2000 sites.

In Fig. 5, we measure the density-density correlations at a time  $\tau=600$ , at which the initial Fock state has already completely melted. Figure 5(d) shows the density profile at this time and from that plot, we see that at time  $\tau=600$ ,  $i \approx 705$  separates the front of fast particles from slower ones, as indicated by the vertical dashed line in the figure. Panels (a) and (b) show  $|N_{ij}|$  for  $i>j$ , and  $j=20$  and  $j=740$ , respectively, i.e., measured from behind and from inside the moving front [Fig. 5(d)]. While in the latter case, clearly a unique power-law decay of  $|N_{ij}|$  is observed, the former case is more involved. There, the envelope of the correlator also decays according to  $|N_{ij}|=\alpha|i-j|^\beta$ , yet for  $i \leq 705$  and  $i \geq 705$ , a different prefactor  $\alpha$  is found. These are the two regions in Fig. 5(a) indicated by the arrows. The exponent  $\beta=2K$  is universal and expected to be  $\beta=2$  since the Luttinger parameter  $K$  of spinless fermions is  $K=1$ , but the prefactor—in the ground state—is essentially a function of the average density, or the Fermi momentum, respectively [22]. The density-density correlations therefore exhibit a distinctly different behavior comparing the moving front of fast particles ( $i \geq 705$ ) and those left behind ( $i \leq 705$ ). It is exactly this step-like feature, i.e., the sudden change in the prefactor of the power law followed by  $|N_{ij}|$ , that is not captured by the reference systems. This is revealed in Fig. 5(c), which shows the  $|N_{ij}^{\text{ref}}|$  as measured in the reference system constructed for time  $\tau=600$ , for both  $j=20$  and  $j=740$ . The plot includes the fits to  $|N_{ij}|$  from panels (a) and (b) (dotted-dashed lines). While for  $j=740$ ,  $|N_{ij}|$  is well described by the reference systems,  $|N_{ij}^{\text{ref}}|$  with  $j=20$  does not show the steplike feature observed in the moving cloud, as the reference systems fail to account for the separation of particles moving at different velocities.

For this reasoning to apply, it is important to realize that such a separation of velocities as reflected in the two prefactors to the power-law decay is not observed in the expansion from a TL state. There, a power law with a single pair of exponent and prefactor governs the decay of one-particle and density-density correlations [16].

### E. Nonintegrable systems

Beyond the case of the Hubbard model Eq. (1), the question arises whether nonstationary states of other model Hamiltonians may as well be described by ground-state reference systems. Conceptually, one may wonder whether integrability plays a role or not.

While a full account of these interesting issues is beyond the scope of the present work, we wish to at least comment on one additional model, the extended Hubbard model. In addition to the terms given in Eq. (1), this model incorporates a nearest-neighbor repulsion  $H_2$  as follows:

$$H_2 = V \sum_{l=1}^{N-1} n_l n_{l+1}. \quad (7)$$

The nearest-neighbor interaction both renders the system nonintegrable and induces additional phases at half-filling.

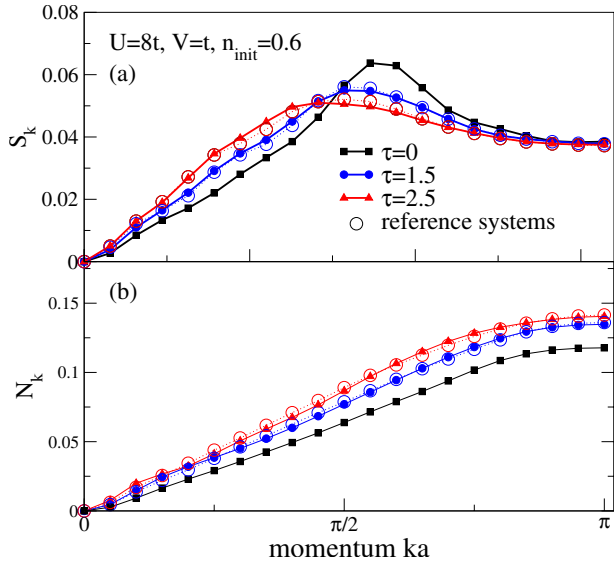


FIG. 6. (Color online) Structure factor for (a) spin and (b) density correlations for the extended Hubbard model with  $U=8t, V=t$ . The results are for the expansion from an initial state with  $n_{\text{init}}=0.6$  and 6 particles. Time-dependent data are represented with solid lines and solid symbols; the corresponding ground-state reference system ones are displayed with open circles.

For  $V < U/2$ , the system is a Mott insulator, while a large  $V$  drives the system into a charge-density-wave phase [28]. Here we focus on the numerically less demanding case of the expansion from an initial state with an incommensurate filling of  $n_{\text{init}}=0.6$ . We postpone the discussion of the MDF to a future publication, but rather compute the spin and charge structure factors for both the expanding system and the reference systems constructed according to the prescription of Sec. IV A. The results for  $U=8t$  and  $V=t$  are collected in Fig. 6, and we note that in this case, we consider the expansion from a box trap only.

Our observation is that the reference systems still provide a very good approximation to the time-dependent correlations. Moreover, the agreement remains much better for the spin structure factor than for the charge structure factor. Future work will have to clarify whether the reference system description breaks down as  $V$  is increased. In conclusion, we find that the reference system description does not seem to be crucially dependent on integrability, and we expect a similar picture to emerge in other models.

#### F. Discussion: Relation to density functional theory

Our main results have shown that starting from a Mott insulator, the temporal evolution of spin and density correlation functions are very accurately described by the ground state of reference systems defined at each instant of time so that they have the same density distribution as the time-evolving system. Such a description deteriorates after the

Mott insulating region has totally melted. On the other hand, for systems starting with densities  $n_{\text{init}} < 1$ , the description with reference systems remains valid up to the largest times reached in our simulations. These results explicitly show that the correlation functions studied here are functionals of the density, a fact that is in accordance with density functional theory (DFT) for time-dependent systems [29,30].

DFT considers, both for the ground state and time-dependent situations, this kind of Hamiltonian [29,30]:

$$H = H_{\text{kin}} + H_{\text{Coulomb}} + H_{\text{ext}}, \quad (8)$$

i.e., one separates the Hamiltonian into kinetic energy, the interaction energy due to Coulomb interactions, and an external potential. We should here remark that in our case, the time-dependent external potential is discontinuous at time  $\tau=0$ , as we use  $H_{\text{ext}}=H_{\text{conf}}$  at time  $\tau=0$  and  $H_{\text{ext}}=0$  for  $\tau>0$ . Therefore, it does not strictly comply with the assumptions needed to prove the Runge-Gross theorem [31], i.e., the external potential needs to be analytical around  $\tau=0$ .

However, and most importantly, the reference systems explicitly provide the required functionals, namely, the correlation functions in the respective ground states. This is, to our opinion, a rather surprising and nontrivial fact that the correlations of a genuinely nonstationary state can be quantitatively described by equilibrium systems. Moreover, since they are in their ground state, this suggests that a minimum principle is at work here. As shown in Sec. IV E, these conclusions are not restricted to the pure Hubbard model, i.e., they are not a consequence of integrability. Therefore, we expect that they hold in general.

#### V. SUMMARY

In this work, we have identified several remarkable and unexpected properties of fermions expanding into an empty lattice. These include the emergence of coherence as well as an accumulation of particles at momentum  $\pi/2$  in the expansion of particles coming from a MI region. In particular, we have shown that correlation functions of expanding, interacting fermions can be accurately described by equilibrium reference systems in their ground state. These results are expected to qualitatively carry over to other models as well, and certainly also apply to the case of hard-core bosons.

#### ACKNOWLEDGMENTS

We thank A. Kolezhuk, A. Leggett, and D. Scalapino for fruitful discussions. F.H.-M. and E.D. were supported in part by NSF Grant No. DMR-0706020 and the Division of Materials Science and Engineering, U.S. DOE, under contract with UT-Battelle, LLC. M.R. was supported by NSF Grant No. DMR-0706128 and Department of Energy Grant No. DOE-BES DE-FG02-06ER46319. A.M. acknowledges partial support by DFG through Grant No. SFB/TRR21.

- [1] I. Bloch, J. Dalibard, and W. Zwerger, e-print arXiv:0704.3011, *Rev. Mod. Phys.* (to be published).
- [2] T. Kinoshita, T. Wenger, and D. S. Weiss, *Nature (London)* **440**, 900 (2006); S. Hofferberth, I. Lesanovsky, B. Fischer, T. Schumm, and J. Schmiedmayer, *ibid.* **449**, 324 (2007).
- [3] M. Greiner, O. Mandel, T. W. Hänsch, and I. Bloch, *Nature (London)* **419**, 51 (2002).
- [4] H. Moritz, T. Stöferle, M. Köhl, and T. Esslinger, *Phys. Rev. Lett.* **91**, 250402 (2003); H. Ott, E. de Mirandes, F. Ferlaino, G. Roati, G. Modugno, and M. Inguscio, *ibid.* **92**, 160601 (2004); C. D. Fertig, K. M. O'Hara, J. H. Huckans, S. L. Rolston, W. D. Phillips, and J. V. Porto, *ibid.* **94**, 120403 (2005); J. Mun, P. Medley, G. K. Campbell, L. G. Marcassa, D. E. Pritchard, and W. Ketterle, *ibid.* **99**, 150604 (2007); N. Strohmaier, Y. Takasu, K. Günter, R. Jördens, M. Köhl, H. Moritz, and T. Esslinger, *ibid.* **99**, 220601 (2007).
- [5] M. Rigol, V. Dunjko, V. Yurovsky, and M. Olshanii, *Phys. Rev. Lett.* **98**, 050405 (2007); M. Rigol, A. Muramatsu, and M. Olshanii, *Phys. Rev. A* **74**, 053616 (2006).
- [6] M. A. Cazalilla, *Phys. Rev. Lett.* **97**, 156403 (2006).
- [7] P. Calabrese and J. Cardy, *Phys. Rev. Lett.* **96**, 136801 (2006).
- [8] P. Calabrese and J. Cardy, *J. Stat. Mech.: Theory Exp.* (2007) P06008.
- [9] C. Kollath, A. M. Läuchli, and E. Altman, *Phys. Rev. Lett.* **98**, 180601 (2007).
- [10] S. R. Manmana, S. Wessel, R. M. Noack, and A. Muramatsu, *Phys. Rev. Lett.* **98**, 210405 (2007).
- [11] V. Eisler and I. Peschel, *J. Stat. Mech.: Theory Exp.* (2007) P06005; V. Eisler, D. Karevski, T. Platini, and I. Peschel, *ibid.* (2008) P01023.
- [12] M. Cramer, C. M. Dawson, J. Eisert, and T. J. Osborne, *Phys. Rev. Lett.* **100**, 030602 (2008).
- [13] M. Eckstein and M. Kollar, *Phys. Rev. Lett.* **100**, 120404 (2008).
- [14] T. Barthel and U. Schollwöck, *Phys. Rev. Lett.* **100**, 100601 (2008).
- [15] M. Rigol and A. Muramatsu, *Phys. Rev. Lett.* **93**, 230404 (2004); K. Rodriguez, S. R. Manmana, M. Rigol, R. M. Noack, and A. Muramatsu, *New J. Phys.* **8**, 169 (2006).
- [16] M. Rigol and A. Muramatsu, *Phys. Rev. Lett.* **94**, 240403 (2005); *Mod. Phys. Lett. B* **19**, 861 (2005).
- [17] A. Micheli, A. J. Daley, D. Jaksch, and P. Zoller, *Phys. Rev. Lett.* **93**, 140408 (2004); A. Micheli and P. Zoller, *Phys. Rev. A* **73**, 043613 (2006).
- [18] B. Horstmann, J. I. Cirac, and T. Roscilde, *Phys. Rev. A* **76**, 043625 (2007).
- [19] D.M. Gangardt and M. Pustilnik, *Phys. Rev. A* **77**, 041604(R) (2008).
- [20] A. Minguzzi and D. M. Gangardt, *Phys. Rev. Lett.* **94**, 240404 (2005).
- [21] H. Buljan, R. Pezer, and T. Gasenzer, *Phys. Rev. Lett.* **100**, 080406 (2008).
- [22] T. Giamarchi, *Quantum Physics in One Dimension* (Clarendon Press, Oxford, 2004).
- [23] S. R. White and A. E. Feiguin, *Phys. Rev. Lett.* **93**, 076401 (2004); A. Daley, C. Kollath, U. Schollwöck, and G. Vidal, *J. Stat. Mech.: Theory Exp.* (2004) P04005.
- [24] M. Rigol and A. Muramatsu, *J. Low Temp. Phys.* **138**, 645 (2005).
- [25] T. Kinoshita, T. Wenger, and D. S. Weiss, *Science* **305**, 1125 (2004).
- [26] D. Clément, A. F. Varón, M. Hugbart, J. A. Retter, P. Bouyer, L. Sanchez-Palencia, D. M. Gangardt, G. V. Shlyapnikov, and A. Aspect, *Phys. Rev. Lett.* **95**, 170409 (2005).
- [27] C. Fort, L. Fallani, V. Guarrera, J. E. Lye, M. Modugno, D. S. Wiersma, and M. Inguscio, *Phys. Rev. Lett.* **95**, 170410 (2005).
- [28] See, e.g., E. Jeckelmann, *Phys. Rev. Lett.* **89**, 236401 (2002).
- [29] R. M. Dreizler and E. K. Gross, *Density Functional Theory* (Springer, Berlin, 1990).
- [30] E. K. U. Gross and K. Burke, *Lect. Notes Phys.* **706**, 1 (2006).
- [31] E. Runge and E. K. U. Gross, *Phys. Rev. Lett.* **52**, 997 (1984).